Characterization of Damage in Hyperelastic Materials Using Standard Test Methods and Abaqus

[*]Arun U Nair, [**]Hubert Lobo, and [*]Anita M Bestelmeyer

[*] BD, Research Triangle Park, NC 27709, USA

[**] DatapointLabs, Ithaca, NY 14850, USA

Abstract: Over the past couple of decades, standard test methods and material models have existed for rubber-like materials. These materials were classified under the category of Hyperelastic materials. Well established physical test methods and computational procedures exist for the characterization of the material behavior in tension, compression, shear volumetric response, tear strength etc. However, effective modeling of the fracture behavior of hyperelastic materials using finite element techniques is very challenging. In this paper, we make an attempt to demonstrate the use of such standard test methods and the applicability of such test data for performing finite element analyses of complex nonlinear problems using Abaqus. Our goal is to demonstrate the effective use of standard physical test data to model multi-axial loading situations and fracture of hyperelastic materials through tear tests and indentation test simulations.

Keywords: Hyperelastic Material, Damage, Tear Test, Cohesive Elements, Indentation Test

1. Introduction

Hyperelastic materials or rubber-like materials exhibiting very large elastic strains often find profound use in various industries like automotive, consumer products, medical devices etc. Hyperelastic materials are widely used and well established physical testing methods exist for mechanical characterization; however, successful use of such physical test data in finite element analyses is often challenging. These challenges include identification of an appropriate material model and parameters that characterize the specific material behavior. In this respect, Abaqus offers a wide range of hyperelastic material models and robust calibration tools based on curve fitting techniques which can utilize standard material characterization test data. However, analysts often encounter situations where the available material models become incapable of providing a satisfactory fit for all the deformation modes represented by standard physical test procedures for hyperelastic materials. Yet another challenging situation is modeling the failure of hyperelastic materials or situations involving the damage of such materials. Under these circumstances, the selection of an appropriate material model becomes difficult and requires pragmatic approaches. Computational procedures to characterize the damage in hyperelastic materials are often very challenging due to the limitations in the material models and requirements of complex test procedures. Standard and simplistic physical test methods exist for determining the tear strength of rubber-like materials. In this paper, we make an attempt to review standard test methods and applicability of such test data for performing finite element analyses. The damage model used for tear-test modeling was based on the penalty-based cohesive element formulations originally proposed by Diehl, T. (2005, 2008).

This paper is organized into several sections as follows. In Section 1, we review the experimental procedures for characterizing the mechanical behavior of hyperelastic materials with an emphasis on the equivalency between different tests and estimation of tear strength. Specifically we used the physical test data from a standard tear test to determine the critical fracture energy using cohesive elements adopting an inverse approach. Section 2 presents the methodology for calibrating the material constants for cohesive elements and tear test simulation and model validation. Sections 3 and 4 present the results and model details of the indentation test, which represents a multi-axial loading case. Conclusion of these studies is outlined in Section 5.

2. Experimental Techniques

2.1 Hyperelastic material model calibration

The material used in this work was commercially available polyurethane sheets. The sample was provided in sheet form, 12” square and 1/16” thick. Test specimens were punched or cut into the desired forms as needed. Specimens were not pre-cycled prior to testing to maintain compatibility between the material model and the simulation of the actual end use case. In the actual case to be simulated, the material in its virgin form was subjected to deformation that resulted in failure. An Instron 5566 universal testing machine was used for all of the testing. Four types of tests were performed to characterize the different modes of deformation of the rubber. Tensile experiments were performed using standard ASTM D412 tensile bars. Video extensometry was used for the strain measurements.

The shear behavior of the rubber was characterized using the planar tension test. The aspect ratio used was 4” wide and 1” high. Again, no pre-cycling was used. Biaxial behavior was measured using two means. Lubricated compression experiments were conducted using stacked specimens [1]. 1” diameter disks were punched from the sheet and these were stacked to create test specimens about 0.4” (10 mm) high. These were placed between silicon oil lubricated platens and subjected to compressive loading. The stress strain data, expressed in engineering form, is presented in Figure 1 below. To aid in the presentation of the data, the compressive data was converted to a biaxial form using the following equations:

$$\varepsilon_b = \sqrt{(1/(\varepsilon_c + 1)} - 1 \qquad (1)$$

$$\sigma_b = \sigma_c//(\varepsilon_c + 1)^3 \qquad (2)$$

where,

σ_c = compressive engineering stress (psi)

ε_c = compressive engineering strain (unitless)

σ_b = biaxial engineering stress (psi)

ε_b = biaxial engineering strain (unitless)

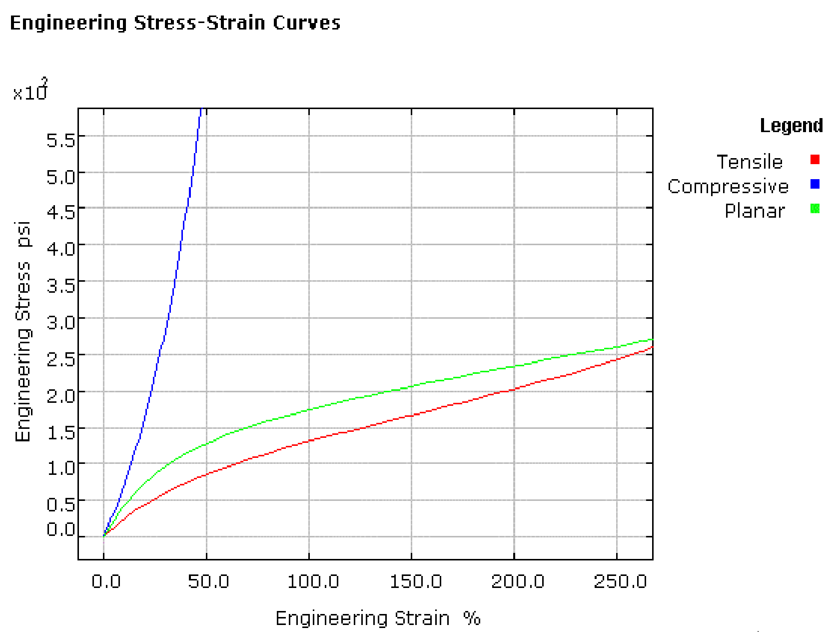

Figure 1. Hyperelastic data for the rubber

Biaxial properties were also measured using a cruciform fixture. This fixture takes a test specimen of square cross section and stretches it equibiaxially in the x and y directions. The fixture is placed in the Instron 5566 UTM. Strain is measured directly using video extensometry. Measured load is converted to stress using the following equation:

$$\sigma_b = F_b/(2\ lt) \tag{3}$$

where,

F_b = biaxial force (Lbf)

l = length of one side of the cruciform specimen

t = thickness of the cruciform specimen (mm)

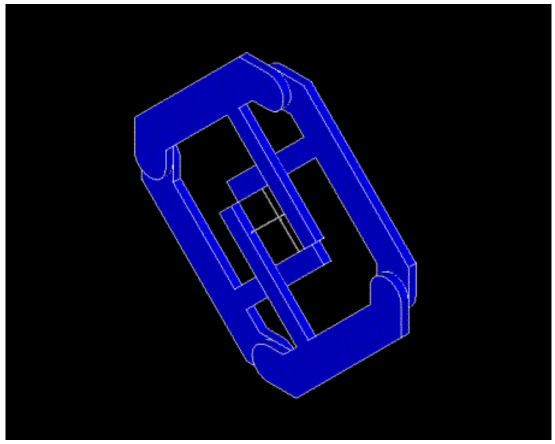

Figure 2. Cruciform biaxial test fixture

Hyperelastic theory shows that tensile and compressive data are equivalent. Experimental limitations can prevent this equivalence from being observed in practice. In this work, we are able to show that lubricated compressions and equibiaxial test data yield similar results and can be used interchangeably for hyperelastic modeling. Figure 2 below shows a comparison plot between the two techniques for the polyurethane.

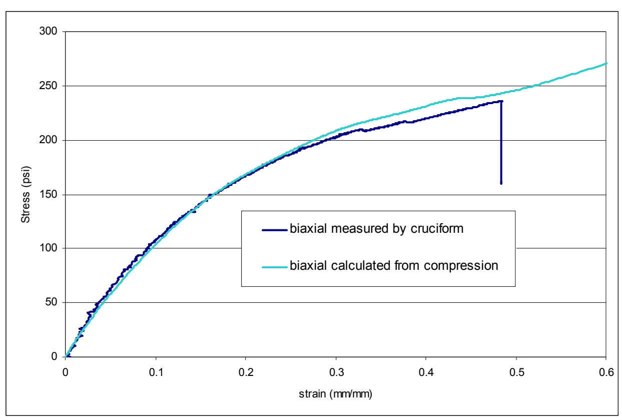

Figure 3. Comparison of equibiaxial tension and lubricated compression

2.2 Tear test

Tear tests are commonplace in the testing of rubber, providing a simple means to evaluate the failure characteristics of rubber materials. Test specimens have been specifically designed for this purpose. We selected the ASTM D624 Type C test specimen also called the bow-tie specimen. This specimen has a 90 degree angle on one side and is rounded on the other resulting in a specific location for damage initiation and tear propagation. The force acts on the specimen in a direction essentially parallel to the direction of the grip separation. Failure is generally linear and occurs perpendicular to the direction of grip separation, an important consideration for the subsequent simulation work. The test was performed at a speed of 19.7 in/min. In addition to the tear strength, the load vs. displacement data was also gathered and is shown below in Figure 4.

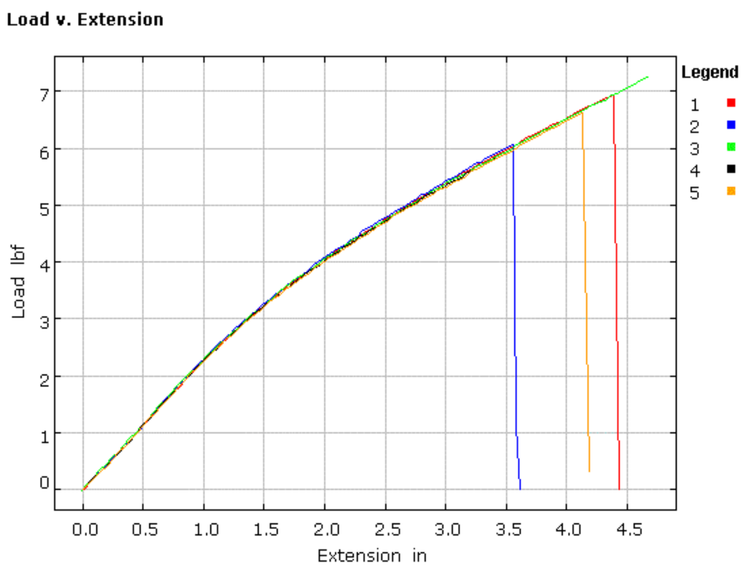

Figure 4. Load-displacement from a bow-tie tear test

3. Tear Test Model

Tear strength is an important mechanical characteristic for determining the resistance to fracture or inducing damage in hyperelastic or rubber-like materials. Several standard test procedures exist for estimating the tear strength of hyperelastic materials. Clamroth & Kempermann (1986) have presented a comprehensive review of several tear test methods, their relevance and a comparison between the various test methods. One of the very commonly used tear test procedures is the ASTM Type C Tear test (ASTM – D624 – Type C Tear Test). Such standardized test procedures have been in place for over several decades, yet developing finite element models to simulate crack initiation and propagation in hyperelastic material has been very challenging. This highly nonlinear problem is further complicated by the material damage or crack initiation and propagation that occur during the actual tearing process.

To the best of our knowledge, a very limited capability exists in commercial FEA codes to model the damage which occurs in hyperelastic materials. The primary value of interest in studying the fracture behavior of materials is the critical fracture energy or the critical energy release rate. Critical fracture energy characterizes the energy the material releases per unit crack growth. In this section, we are proposing a finite element based technique using cohesive elements in Abaqus to estimate fracture energy in conjunction with the physical test data from a standard ASTM Type C tear test. We propose an inverse approach for estimating fracture energy. The properties of cohesive elements using a traction separation material model was iteratively varied to minimize the error between the force-deflection curve obtained from the finite element model and the physical test data for a generic hyperelastic material. It may be noted that this technique is applicable only to hyperelastic materials failing through a straight crack at the mid section of the test specimen.

3.1 Damage Model and Penalty Approach for Cohesive Elements

In the present study, we have used a penalty based cohesive element approach to model the crack propagation and failure of the tear test specimen. We have used the penalty based approach for cohesive elements in Abaqus originally proposed by Diehl, T. (2005, 2008). Cohesive element response is based on energy principles and for this study we have used a *traction separation* material law for modeling the crack initiation and propagation during the tear test. A very detailed description of cohesive elements, their behavior and modeling techniques can be found in Diehl, T. (2005). A single parameter G_c (critical fracture energy) with BK mixed mode behavior was chosen due to its simplicity and isotropic material behavior.

With an isotropic assumption, G_c values are set to the same values for Mode I, Mode II and Mode III. This results in the triangular law shown below in Figure 5. This implies that the stress to failure and effective modulus will have the same values for out-of plane and two in-plane directions. For the use of traction separation behavior and associated cohesive element failure, one needs to specify three distinct phases of the material behavior namely, elastic response prior to any damage initiation, criteria for damage initiation and criteria for damage evolution. During the tear test, until the initiation of a tear or crack, the material is assumed to be bonded together with an infinite bond strength at the interface. For this study, we have adopted the single parameter penalty based approach proposed by Diehl, T. (2005). Only a brief description of various relationships used for setting up cohesive element is given below, for the sole purpose of completeness. For a more detailed description of this implementation, please refer to Diehl, T. (2005).

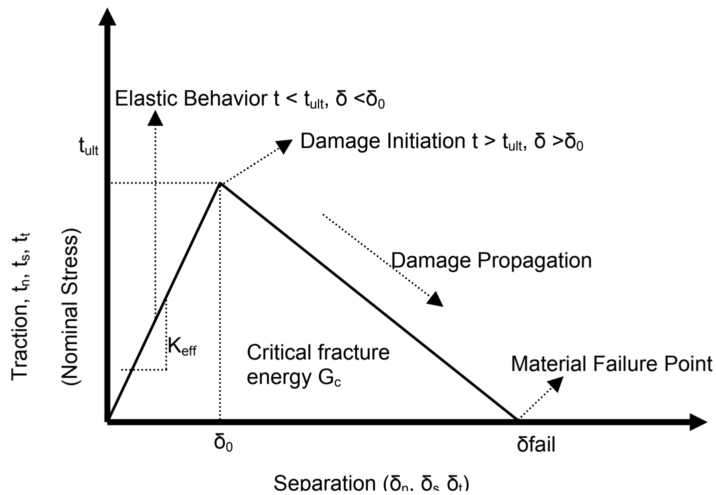

Figure 5. Traction separation law

From Figure 5, we can write the expression for critical fracture energy G_c as

$$G_c = \frac{t_{ult}\delta_{fail}}{2} \tag{4}$$

In the above expression, t_{ult} represents the maximum stress value and δ_{fail}, the separation corresponding to failure of the material. The subscripts "*n, s and t*" in Figure 5 represent the out-of-plane and two in-plane directions, respectively, for a 3D model. Ideally, we want the cohesive elements that bond the *tear test* specimen together to be infinitely rigid, but this may give rise to numerical problems. So we have kept δ_{fail} to 0.05 times the characteristic cohesive element dimensions in the model. Therefore, for a known value of G_c, the maximum stress to failure can be determined. It may be noted that this is not the actual failure stress value for the material, but instead a penalty term based on the assumed value for separation at failure δ_{fail}. For this study, our goal is to determine a G_c value from the tear test data. Therefore, for the initial case, we will have to assume a G_c value and iteratively vary it in such a way that the predicted force-deflection curve from the finite element model is in very good agreement with the force-deflection curve obtained from the physical test. Having obtained G_c and t_{ult} values from the material property data and eqn (4), we can specify the *damage initiation* and *damage propagation* criteria for cohesive elements.

We must define the linear elastic material behavior prior to *damage initiation*. This material behavior is specified as an effective elastic modulus E. Effective modulus is related to the initial stiffness through the following relationship

$$E = K\,h_{coh} \tag{5}$$

where, h_{coh} is the initial effective thickness of the cohesive element. For this study, we have specified the cohesive element thickness as unity so that the effective stiffness and Elastic modulus are equivalent. From Figure 5, we can write the initial stiffness K as

$$K = \frac{t_{ult}}{\delta_0} \tag{6}$$

Now we can write the separation corresponding to *damage initiation* δ_0 as a fraction of the separation corresponding to failure δ_{fail} as

$$\delta_0 = \beta\delta_{fail} \tag{7}$$

where β is a scaling factor which can take any value greater than zero and less than one. For this study a value of 0.05 was chosen through modeling studies. Now combining equations (4), (6) and (7) we can write K as

$$K = \frac{2G_C}{\beta\delta_{fail}{}^2} \tag{8}$$

For a unit cohesive element thickness, the elastic modulus will be same as the effective stiffness. The only other parameter that was required for this study was the material density value for the cohesive element. Since the cohesive elements here are used to define the crack propagation direction or fictitious bond line, the concept of density was not realistic. However, for Abaqus Explicit procedures, it is mandatory to specify density values. For this application, the concept of density can be just considered as a parameter with little physical significance. Therefore, our goal was just to identify a density value which would have a negligible effect on the solution quality and at the same time not adversely affecting analysis run times. We identified a density value which kept the analysis run times reasonable and also resulted in no impact on the predicted load-deflection behavior.

3.2 Details of Abaqus Model

A 3D model was used here to simulate the *tear-test* even though a 2D model would have been sufficient. This was mainly due to two reasons. The first reason was to determine the need for changes in parameters used for the penalty based approach originally proposed by Diehl, T. (2005) for 3D models. The second reason was that this modeling study was undertaken as a precursor to more complicated damage problems involving multi-axial loading cases and geometries which cannot be approximated by 2D models. In this way, the penalty parameters determined here can be extended to other 3D models. For this study, we used the geometry of the *ASTM D624 – Type C Tear Test* specimen geometry (see Figure 6). Since this modeling study was used to replicate the *tear-test*, we used boundary conditions that would mimic the test set-up. The specimen was held fixed leaving the effective gauge length unconstrained as shown in Figure 6. We used kinematic coupling constraints to hold the specimen. This was the preferred method as the boundary conditions could be specified at a single point known as a control point or *reference point* and all the regions coupled to this point would exhibit similar kinematic behavior. Through this technique, a user needs to request output for only this control point for estimating the reaction force and displacement related quantities as opposed to requesting output for an entire node set. This approach will significantly reduce the output data and post-processing procedures like filtering.

We used a single invariant based Marlow model to capture the hyperelastic material behavior. The material model was calibrated using the uniaxial tensile data. Several other material models were considered using the planar and compressions test data but the Marlow model gave the best match to the uniaxial tension data. Considering the deformation mode for this problem, it is essential to have a material model that can fit the uniaxial tension data in an exact manner for the required strain levels. As will be shown later, for both of the examples considered here, the Marlow representation gave very good results. The geometry was modeled as two parts stitched together using cohesive elements along the symmetry plane. This plane will represent the crack propagation plane assuming a straight line in-plane crack as observed from the physical test (See Figure 6). Initially, the geometries are bonded through cohesive elements and will respond as a single entity until the criteria for material failure/crack propagation is met as outlined in Section 3.1.

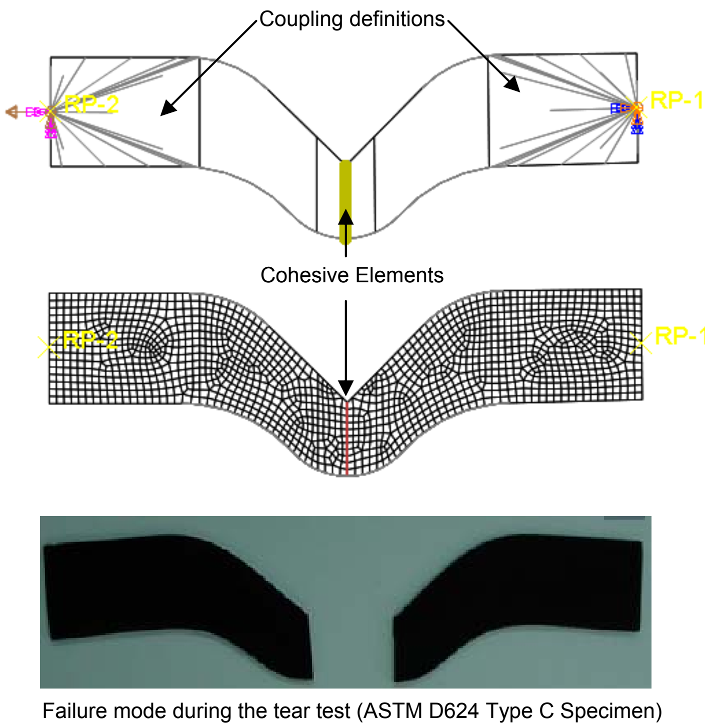

Figure 6. Specimen geometry, boundary conditions, finite element mesh and the failure mode of the specimen during the tear test

Considering the highly nonlinear and unstable nature of the structural response associated with tearing, we chose Abaqus Explicit as the solution procedure. Based on our experience, Abaqus Explicit is more robust in handling such material behavior as compared to implicit solution procedures (Abaqus Standard). It may be possible to model this particular structural response using an implicit method (Abaqus Standard) with appropriate energy dissipation mechanics like stabilization controls and viscous regularization; however, we did not explore this option. We used an initial guess for the G_C value and subsequently iterated until the predicted force-deflection matched the force-deflection curve obtained from the physical test. To ensure realistic model run times, we used mass scaling to speed up the solution ensuring that there were no significant inertial effects. Typically, this check can be done by comparing the kinetic energy values, internal energy and total energy values of the entire model.

3.3 Results

An analysis was performed with the objective being to back-calculate critical fracture energy (G_C) in an iterative manner and to assess the ability of the model to represent the force-deflection behavior obtained from a *tear-test*. Figure 7 shows the comparison of the force-deflection curve predicted by FEA using a G_C value of 0.054 lbf/in determined iteratively. It can be seen that the determined G_C value was able to predict the force-deflection curve and simulate the *tear-test* accurately. The force-deflection curve shown here is a representative sample; however, there will be variations in the maximum load corresponding to material failure between samples. This is to be expected for any material and especially for materials exhibiting large deformations prior to failure. Therefore, the G_C values determined will have some variability and should not be considered exact.

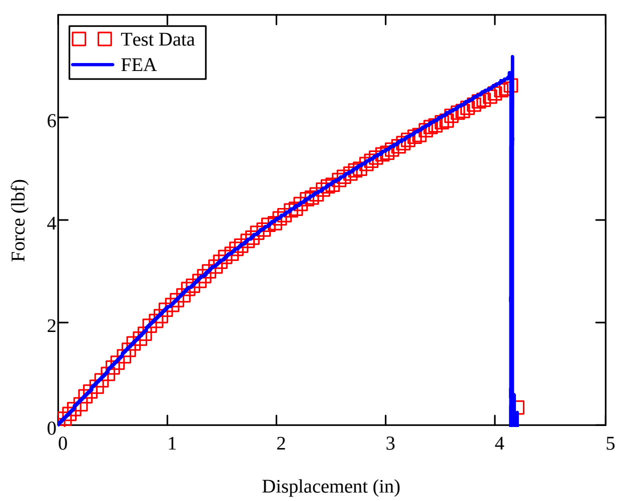

Figure 7. Comparison of force-deflection behavior obtained from FEA and physical test

Based on the specific application, this value might need more fine tuning. Analytical determination of G_C values for materials exhibiting highly nonlinear behavior and associated finite strain behavior is not straightforward. This calls for approximate, yet effective numerical techniques. Procedures like this should be looked upon as a good starting point for more complex real-life damage predictions. The predicted force-deflection curve shows a near exact match with the force-deflection curve determined from the *tear-test* experiment. Results obtained here demonstrate successful extension of the penalty based approach for cohesive elements in Abaqus originally proposed by Diehl, T. (2005) to determine the critical fracture energy of a certain classes of hyperelastic materials.

The excellent agreement observed here is due to the nature of the material fracture (straight crack) and catastrophic failure observed in the physical test. It may be noted that the technique proposed here is valid only if the crack path is very well established and is used as model input data. We did not perform extensive sensitivity studies as part of this study to determine the impact of all the cohesive element penalty parameters as it was very well established in the work by Diehl, T. (2005). A more detailed modeling study shall be undertaken in the future to accommodate more general loading conditions and to assess the ability of these techniques to predict other failure modes in hyperelastic materials.

4. Indentation Test

In the previous section, we demonstrated the use of the standard *tear-test* data for identifying the fracture properties through an inverse approach. In this section, we present a multi-axial loading scenario where we use the same material model used in the previous example. The multi-axial loading scenario we have considered for this study is the indentation of a sheet of hyperelastic material using a gage pin of 0.03 inches in diameter. The goal of this section is to demonstrate the successful use of a standard material test and the Marlow material model for a general loading scenario in addition to its application in determining fracture response. We have chosen the indentation test because of its gaining popularity in the field of biomechanics for determining material properties of soft tissues. There are several articles describing indentation test based material property determination techniques so we are limiting our study here in predicting the load-deflection characteristics. To validate the finite element predictions, we have compared the model predictions against physical test data for a gage pin indentation on a sheet of hyperelastic material. The loading scenario investigated was a highly nonlinear problem involving finite strains and complex contact conditions at the gage pin-sheet interface.

The physical test procedure consisted of a sheet 0.0625 inches thick, which was clamped between two rectangular platens with a circular opening. An adequate clamping force was exerted through mechanical screws. Since this test was conducted just for model validation purposes, advanced clamping mechanisms like pneumatic clamps and clamping force measurement systems were not used. The clamping force was adjusted to minimize slippage of the test specimen. It was observed during clamping screw adjustments that excessive clamping forces could lead to a “bubble” effect in the specimen due to radial compression. This could lead to significant changes in the load deflection behavior during the indentation test. While performing the experiments, the loading was terminated prior to any material failure. During the test, significant material thinning and material "wrap-around" was observed in the contact region.

4.1 Details of Abaqus Model

We have used an implicit scheme (Abaqus Standard) for the simulation and prediction of load-deflection characteristics for the indentation test. Since the goal of the study was to demonstrate the validity of the material model for different loading conditions, we ran the model only to limited deflection levels. At large indentation levels, the implicit scheme will fail to converge due to severe element distortions in the vicinity of the contact region. If the required deformation levels are much higher than the ones presented here, more advanced techniques like rezoning methods, explicit solution schemes with adaptive meshing techniques, etc. need to be used to maintain element shapes within the acceptable range. In this modeling study, we have made an attempt to mimic the physical test conditions by accounting for clamping effects and exact test specimen dimensions.

Taking advantage of the symmetry of the test specimen and loading conditions, an axi-symmetric model was used. The stainless steel gage pin was modeled as a rigid cylinder. An analytic rigid surface was used to represent the gage pin as opposed to a discrete rigid surface. A better convergence will be obtained in complex contact problems due to the absence of any facets while representing the geometry as an analytic rigid surface. The hyperelastic material model used for performing the *tear-test* simulation was used here. Clamping fixtures were modeled through prescribed displacements over the area of contact based on the clamp geometry. This approach circumvents the need for having the test fixtures modeled explicitly and associated contact definitions. The test specimen was modeled using hybrid reduced integration axi-symmetric elements with "enhanced hourglass controls" (CAX4RH). The finite element mesh and boundary conditions used for this study are shown in Figure 8. One of the major challenges was modeling the changing contact conditions along with the finite deformation. The default method used by Abaqus Standard, node-to-surface based hard contact behavior, did exhibit convergence problems as the sheet material began to "wrap-around" the gage-pin with increased levels of deflection. Therefore, we used a penalty stiffness method instead of the "hard" contact formulation. The penalty stiffness was scaled by a factor of 100 as the default penalty-stiffness showed penetration. For contact involving a rigid body deforming a soft material, it is possible that the default penalty stiffness may not be adequate in eliminating or minimizing the penetration levels.

Figure 8. Finite element mesh and boundary conditions

In most cases, these penetration levels will not significantly affect the solution, but possible stress inaccuracies may occur with coarse mesh definitions. A more detailed description about penalty based contact modeling and related issues may be found in the Abaqus User's Manual.

Another challenge we encountered during modeling of this loading scenario using the implicit solution scheme was how to address the unstable structural response associated with clamping of the specimen. The clamping forces will put the sheet of material in radial compression which will give rise to an unstable structural configuration corresponding to a zero frequency mode. This behavior will present convergence difficulties with implicit methods. We used the *STABILIZE option to obtain a converged solution in the region of interest. This will provide a volume proportional damping to stabilize the unstable structural response. Adequate care was taken to ensure that the energy dissipated was a very small fraction of the internal energy. Details of usage and recommended procedures can be found in Abaqus User's Manual. In this study, we have used the new stabilization formulation used in Abaqus called "adaptive stabilization". This technique will ensure that the damping factors are applied in a varying fashion unlike a constant damping factor which can adversely affect the structural response.

4.2 Results

The analyses were performed using the modeling techniques mentioned in the above section. For the loading scenario considered here, the deformed configuration and resulting Von Mises stress contours are shown in Figure 9. The initial phase of deformation could be idealized as Hertzian contact. However, as the deformation levels increase, the material enters the finite strain regime along with significant changes in the contact conditions. The loading was applied only to the point where a converged solution was possible without using complex re-meshing techniques. With continuation of the loading, the material will begin to "wrap-around" the gage-pin and appreciable thinning of the sheet material will occur. This would lead to significant mesh distortion and re-meshing techniques would have to be invoked if one were to model the material response to the point at which the pin would pierce through the sheet material. The deformed configuration plots shown in Figure 9 clearly show the initiation of this behavior where the material begins to "wrap-around" the gage-pin causing significant changes in the contact conditions.

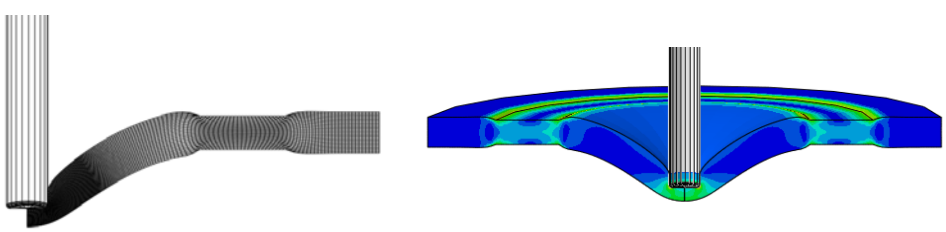

Figure 9. Deformed geometry and Mises stress contours from the Indentation test

Figure 10 shows a plot of the predicted force-deflection curve from FEA along with the force-deflection curve obtained from the physical tests. The red curve represents the averaged curve of all of the test data. It can be noted that the FEA results are in reasonable agreement with the physical test data considering the complex contact conditions and material nonlinearities. It was observed that the few initial increments were influenced by the stabilization factor, which was expected due to the unstable nature of the structure. This kind of unstable behavior can creep into the physical test data as well, appearing as an initial "slack or knee" in the force deflection behavior. In most cases, this behavior is not of interest and hence well established data correction techniques like trimming and extrapolation techniques are employed to remove these effects. The results presented here have been corrected for the initial slack using Kornucopia®, an engineering tool which is very effective for data reduction and post-processing techniques like curve averaging, shifting, extrapolation etc. The slight differences observed here are mainly due to the approximation of the clamping boundary conditions and due to the approximation of the compressive behavior represented using the Marlow model. During the material calibration procedure using the curve fitting techniques within Abaqus, a single material model which fit all of the deformation modes accurately was not found. Hence, we used the Marlow model. We selected the Marlow model because it gave an exact match for the uniaxial tension data and our primary goal was to accurately model the tear test, where the dominant deformation mode was tensile in nature. The results shown here were to demonstrate the applicability of a single invariant dependent Marlow model to capture the structural response for two very different loading scenarios. The solution accuracy may be improved through the simulation of actual test fixtures, determination of exact clamping forces and a more complex material model which gives a more accurate match to the physical test data for all the standard test procedures.

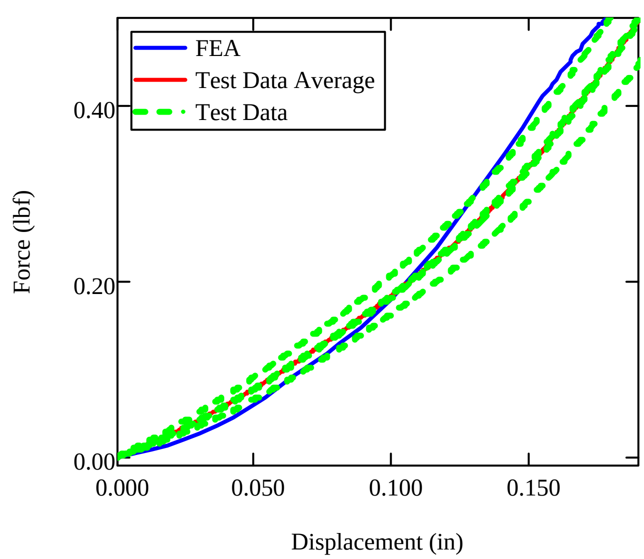

Figure 10. Comparison of force-deflection obtained from FEA and physical tests.

5. Conclusions

We have successfully demonstrated the applicability of modeling techniques using cohesive elements in Abaqus in conjunction with physical test data obtained from a standard *tear-test* to determine the critical fracture energy for a certain class of hyperelastic materials. We have further demonstrated the applicability of the same material model for a general multi-axial loading case through the simulation of the indentation test procedure. Through these examples, it is evident that various, complex structural responses can be modeled accurately using the well established physical test procedures and the hyperelastic material modeling capabilities within Abaqus. This study successfully extended the penalty based modeling techniques using cohesive elements in Abaqus, originally proposed by Diehl, T. (2005, 2008) for modeling failure in surface-bonded structures to determine fracture properties of a certain class of hyperelastic materials. Successful use of this technique would require prior knowledge of the crack propagation direction. The fracture properties determined using the inverse approach presented here can then be utilized to model failure for other loading cases. It may be noted that the major limitation of this approach is that the crack can propagate only along a predefined direction. Finally, this study demonstrated the capability of a single invariant dependent hyperelastic material model (Marlow model) to accurately capture a highly nonlinear and discontinuous material response utilizing standard tensile test data.

6. References

1. Lobo H and Bethard T, “Practical Issues in the Development and Implementation of Hyperelastic Models”, Abaqus Conference Proceedings (2001)
2. ASTM Standard D624, v9.1, pg 141 (1999).
3. Diehl, T., “Modeling Surface-Bonded Structures with ABAQUS Cohesive Elements: Beam-Type Solutions”, Abaqus Conference Proceedings (2005).
4. Diehl, T., “On using a penalty-based cohesive zone finite element approach, Part I: Elastic solution benchmarks”, Journal of Adhesion and Adhesives, vol 28, pp 237-255, (2008).
5. Clamroth, M., Kempermann, Th., “Comparison of Methods for the Determination of Tear Strength”, Polymer Testing, vol 6, pp 3-35, 1986.
6. Abaqus 6.8.1 User’s Manual, (2008).

7. Acknowledgements

We would like to acknowledge the contributions of Jim Pye, Krishna Kulkarni, Ed Lee and Dilip Subramanyam of BD for valuable discussions and generation of experimental data for indentation tests, which were used for validating the finite element model. We would also like to acknowledge the contribution of Brian Croop of DatapointLabs for working through the calculations related to the comparisons between the equibiaxial and compressive measurements and valuable comments about the test methods used in the development of the hyperelastic data.